

*Letter to the Editor***Cold dust in the Andromeda Galaxy mapped by ISO***M. Haas¹, D. Lemke¹, M. Stickel¹, H. Hippelein¹, M. Kunkel¹, U. Herbstmeier¹, and K. Mattila²¹ Max-Planck-Institut für Astronomie, Königstuhl 17, D-69117 Heidelberg, Germany² Helsinki University Observatory, P.O. Box 14, FIN-00014 Helsinki, Finland

Received 20 July 1998 / Accepted 3 August 1998

Abstract. A complete 175 μm map of the Andromeda galaxy (M31) at 1/3 resolution shows the distribution of cold dust. It is dominated by a ring at 10 kpc radius supplemented by a faint outer one at 14 kpc. No clear spiral pattern is recognizable. The azimuthally averaged radial brightness profile is rather flat within the 10 kpc ring and decreases exponentially outside thereof, discernible down to a brightness of 0.07 MJy/sr at a distance of 22 kpc. Since the ring comprises a large reservoir for star formation, as an evolutionary conjecture M31 might be in a transition phase changing its classical optical Sb type spiral morphology towards that of a ringed galaxy.

The bulk of the dust has a temperature of only 16 K, considerably colder than the 21–22 K previously inferred from the IRAS data and also colder than the 19 K found for the Milky Way. The cold dust is accompanied by warm dust, formally described by a component at about 45 K. At the common resolution of 2/5 the triplet 60/100/175 μm flux ratio varies only little across the rings as well as the disk, thus everywhere in M31 at least two dust components are required to fit the far-infrared spectral energy distribution. This provides a direct evidence in M31 for the existence of two dust populations – small and large grains – similar to what had been found in the Milky Way.

For the cold dust component around 16 K we can now estimate the corresponding mass from its emission yielding $3 \cdot 10^7 M_{\odot}$, a dust mass about a factor of ten higher than inferred from the IRAS 60/100 μm data alone. The new cold dust mass – if evenly distributed in the plane of the galaxy – would be sufficient to make the disk of M31 moderately opaque in the optical (face-on: $0.1 M_{\odot} \text{pc}^{-2}$ corresponding to $\tau_V \approx 0.5$).

Key words: infrared: galaxies – galaxies: local group – photometry – ISM: fundamental parameters – individual: M31

Send offprint requests to: M. Haas (e-mail: haas@mpia-hd.mpg.de)

* Based on observations with ISO, an ESA project with instruments funded by ESA Member States (especially the PI countries: France, Germany, the Netherlands and the United Kingdom) and with the participation of ISAS and NASA.

1. Introduction

Two topics guide much of the current research on interstellar dust in spiral galaxies: (1) How opaque are the spiral disks (Disney et al. 1989; Valentijn 1990)?, and (2) what is the total mass of interstellar dust and how much does the cold dust contribute to it? While warm and cool dust at temperatures above 20 K has been well investigated in galaxies (Soifer et al. 1987, Telesco 1993), the observations concerning cold dust at 10–20 K with an expected blackbody maximum around 150–200 μm are still scarce. Since the infrared energy distribution of M31 is steeply rising between 60 and 100 μm , measurements beyond 100 μm are needed to prove the existence of cold dust and to reveal its distribution and its contribution to the mass and opacity of the galaxy.

2. Observations and data reduction

The 175 μm raster map was obtained in February 1997 with ISO's photometer ISOPHOT (Lemke et al. 1996) covering $3^{\circ} \times 1^{\circ}$ oriented along the major axis at PA 39° including the whole galaxy as well as adequate background area. To supplement the spectral informations, stripe-like maps ($75' \times 6'$ parallel to the minor axis) across the center and $22/5$ southwest thereof were secured at various wavelengths between 120 μm and 200 μm .

The data were processed and flux calibrated using the PHOT Interactive Analysis tool PIA¹ V7 in standard processing mode, together with the calibration data set V4 (Laureijs et al. 1998). The final map was produced with the drizzle algorithm (Fruchter & Hook 1997) and restored to about 1/3 FWHM resolution (0.27 kpc at 690 kpc distance) with a photometry-conserving Lucy-Richardson algorithm (Hook et al. 1994).

The photometric accuracy is mainly constrained by the detector response which is measured from the thermal fine calibration source on board. From the partial overlaps of the nine independent submaps (which comprise the whole map) the re-

¹ PIA is a joint development by the ESA Astrophysics Division and the ISOPHOT Consortium led by the MPIA. Contributing Consortium institutes are DIAS, RAL, AIP, MPIK, and MPIA.

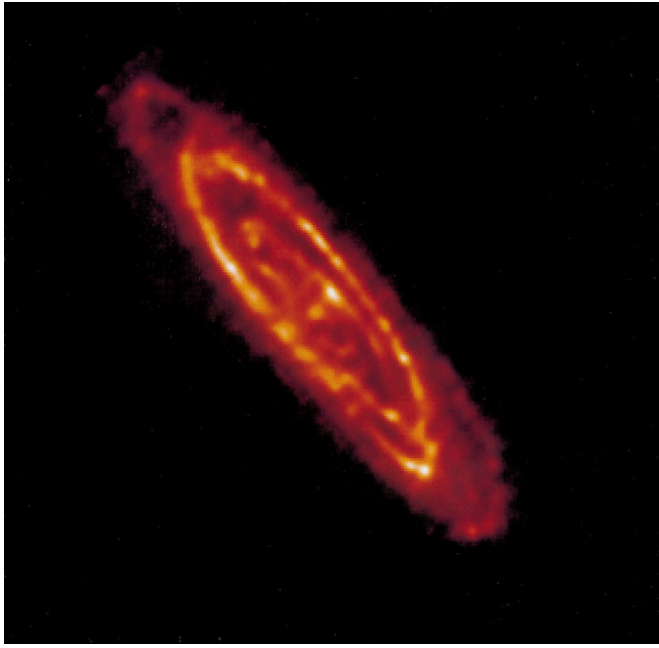


Fig. 1. ISO 175 μm map of M31, north is up, east is left. The emission is dominated by a ring structure at 10 kpc radius (50' along the major axis at PA 39°), with numerous bright condensations and a faint outer ring at 14 kpc. At 175 μm – sensitive to cold emission – the warm nucleus is faint as well.

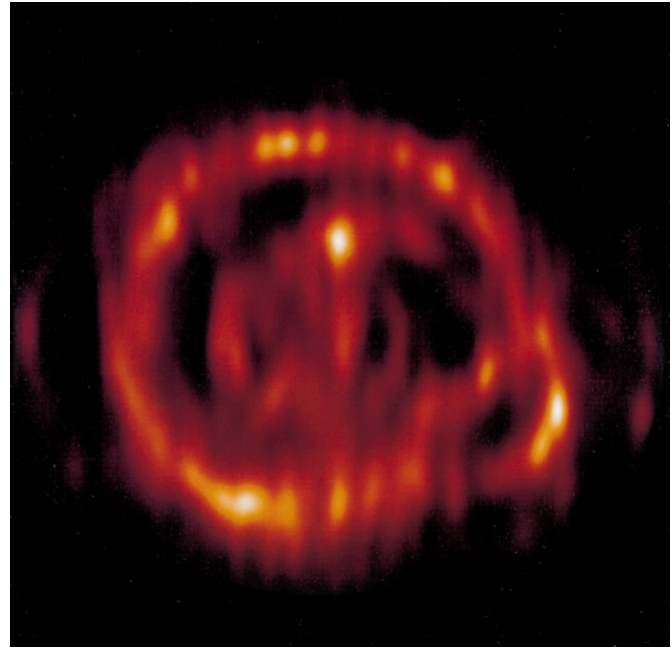


Fig. 2. Face-on deprojection of the 175 μm image of M31, adopting a thin disk and an inclination of 75.5°. The major axis lies horizontally, i.e. north-east is on the left. The structure is dominated by the cold ring at 10 kpc radius. No clear spiral pattern is recognisable. The perturbations in the southwest might be caused by the companion galaxy M32.

producibility is estimated to be better than 10%, thus we consider this value as reasonable error estimate.

3. Results and discussion

3.1. Morphology

The 175 μm map of M31 (Fig. 1) is dominated by an almost complete ring with a major axis radius of 50' (10 kpc). It is resolved into a number of individual knots and has an appearance quite similar to the IRAS 100 μm image (Habing et al. 1984, Walterbos & Schwering 1987, Xu & Helou 1996a). In contrast to the IRAS 100 μm image, at 175 μm the nucleus itself is not the brightest compact source, rather, this is a region about 5' northwest of the nucleus. The most noticeable disturbance of the ring lies at its southwest end, where it appears to be splitted, with three very bright knots lying farthest away from the nucleus. A second fainter and more distant ring is discernible at the southwestern and northeastern end of the galaxy. Inside the bright ring and surrounding the nucleus, several elongated structures are visible, which are reminiscent of another highly disturbed ring. The overall far-infrared morphology of M31 would therefore more consistently be described as a multiple ringed galaxy rather than the Sb spiral type found at optical wavelengths.

A face-on deprojection (Fig. 2) emphasises the bright 10 kpc ring. It has been detected as well in most of the large scale maps in the radio (Beck & Gräve 1982, Brinks & Shane 1984) and is also traced by star forming regions (Pellet et al. 1978, Devereux et al. 1994). Although repeated attempts have been made to investigate the supposed spiral structure of M31 (Arp 1964;

Braun 1991), the results are not convincing. The multiple ring structure can be noted also in the optical via masking (Walterbos & Kennicutt 1988) and in the distribution of HII regions (Pellet et al. 1978), OB associations (van den Bergh 1991), HI gas (Sofue & Kato 1981) and other tracers (see Hodge 1990).

The 10 kpc ring is much brighter at 175 μm than expected from a decomposition of the IRAS 60 μm and 100 μm into a warm and cold dust component (Hoernes et al. 1998). This indicates that the interstellar matter of the 10 kpc ring, the major region of star formation in M31, contains significant amount of cold dust despite the somewhat higher density of the ambient radiation field.

The azimuthally averaged 175 μm surface brightness profile (Fig. 3) is rather flat out to the 10 kpc ring and shows an exponential decrease at larger radii, thereby closely resembling the IRAS 60 μm and 100 μm profiles (see also Bothun & Rogers 1992). Although the central region is densely populated by stars as seen in optical images, most of the interstellar matter – being more dissipative than the stars – must have been effectively removed from that region and possibly transferred to the bright 10 kpc ring. Notably, the Milky Way and the edge-on spiral galaxy NGC 891 as well have a molecular ring at about 5 kpc inside of which the interstellar matter density is less or equal to the ring level.

About one fifth of all spiral galaxies exhibit a ring-shaped pattern in their *optical* light distribution and in many cases the rings could be identified with dynamical orbit resonances associated with a central bar (Buta & Combes 1996). M31 has

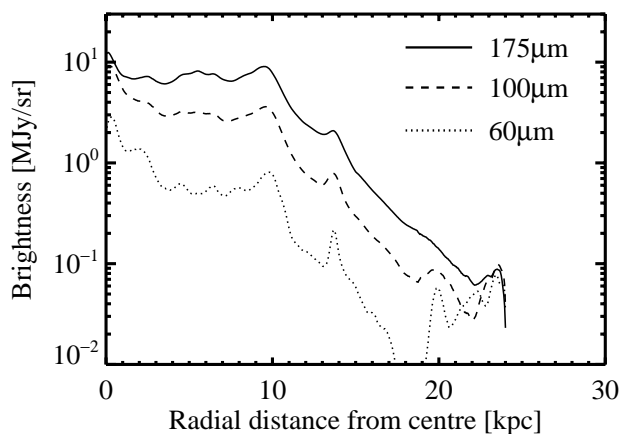


Fig. 3. Azimuthally averaged radial brightness profiles of M31 in the far infrared. In particular at $175\ \mu\text{m}$, it is quite flat inside the bright 10 kpc ring and decreases exponentially outside thereof, recognisable until 22 kpc. The faint outer ring shows up at 14 kpc.

a weak oval distortion in the center (Stark 1977) accompanied with non-circular motions, thus a resonance mechanism could also explain the multiple dust (and gas) rings. They could be formed while the bar was stronger than today, and after the weakening of the bar they could survive. For the flocculent spiral NGC 7217 with three optical and gaseous ringlike zones a similar situation was suggested by Buta et al. (1995). In M31 about 50% of the dust (and most of the gas) is concentrated in the rings, and with more stars being born they will become more prominent at optical wavelengths as well. Thus M31 could be considered as a proto-ringed Sb galaxy, a well suited case for further studies of the ongoing mutative phase.

3.2. Dust properties

The overall infrared spectral energy distribution of M31 rises beyond $100\ \mu\text{m}$, with an integrated ISO $175\ \mu\text{m}$ flux (7900 ± 800 Jy) about more than twice the IRAS $100\ \mu\text{m}$ flux. The spectral energy distributions and temperatures are shown in Fig. 4 for the total galaxy, the nucleus and the stripe maps. The consistency of the photometry is indicated for the nucleus and the stripe maps by the smooth transitions between the IRAS and the ISO data, and for the total galaxy by the nice agreement with the COBE/DIRBE 140 and $240\ \mu\text{m}$ fluxes recently reported by Odenwald et al. (1998). This indicates beyond doubt a major dust component much colder than that inferred from the IRAS observations alone. The cold dust temperature of 16 ± 2 K is determined by the data beyond $100\ \mu\text{m}$. It should be mentioned that an additional very cold dust component below 10 K would show up only beyond $200\ \mu\text{m}$, thus not detectable with ISO. The $60/100/175\ \mu\text{m}$ flux triplet cannot be fitted by a single blackbody and thus it allows for the separation into the cold and warm dust contributions to the global emission. The division into two components is a simplification and it is more likely that there exists a continuous range of temperatures, but there are not yet enough data points to determine the detailed temperature spectrum.

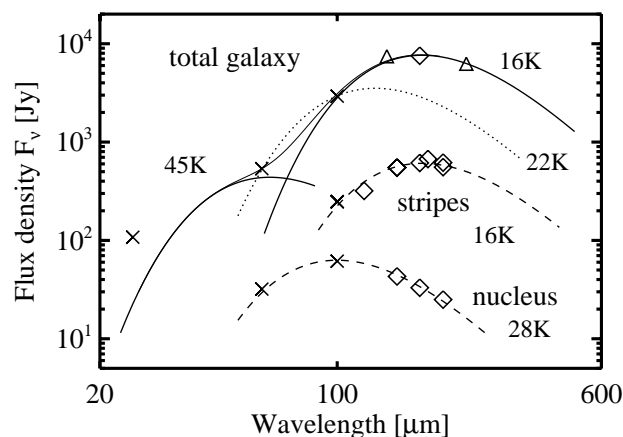


Fig. 4. Infrared spectral energy distribution of M31. The data are shown by symbols (diamonds ISO, crosses IRAS, triangles DIRBE) with the size being larger than the errors. The blackbody curves with emissivity proportional to λ^{-2} are shown by lines. The dotted line with $T = 22$ K through the IRAS 60 and $100\ \mu\text{m}$ data points indicates what one would extrapolate from this wavelength range alone without any further assumptions. The data obtained from the map stripes at various wavelengths clearly determine the shape of the energy distribution. They show that there is actually a maximum around $175\ \mu\text{m}$ corresponding to a temperature of 16 K which fits the total flux as well. With respect to the dominating 16 K curve the flux shows an excess at $60\ \mu\text{m}$, indicating the presence of accompanying warm dust which is here formally described by a 45 K blackbody. The nucleus (4.5×4.5 , 1×4 kpc) – after subtraction of the disk contribution – has a temperature of 28 K.

Next we consider how far the dust temperature varies spatially and how the warm and cold components can be understood. The $100\ \mu\text{m}$ – $175\ \mu\text{m}$ difference map (Fig. 5) spatially separates the cold from warmer areas. The warm areas in the ring coincide with HII-regions. However, for both the warm and the cold areas in the disk and ring (i.e. those showing a positive respectively negative excess in the $100\ \mu\text{m}$ – $175\ \mu\text{m}$ difference map) the spectral energy distributions between 60 and $175\ \mu\text{m}$ exhibit a shape very similar to that of the whole galaxy. For all these areas the spectral energy distribution can not be described with a single blackbody, rather it requires two components. As for the total galaxy, good fits are provided using a 16 K cold and a 45 K warm component with intensity ratios ranging between 100/3 and 100/9 which represents only a moderate (spatial) variation. The essential dust components seem to be the cold and the warm dust which can be seen best at $175\ \mu\text{m}$ and $60\ \mu\text{m}$. This suggests a mixture of small and large dust particles with the diffuse interstellar radiation field as their main heating source. The smaller dust particles are heated to higher temperatures than the larger ones, similar as proposed in the interstellar dust population model (Desert et al. 1990) for the Milky Way. While previous dust studies of M31 (Walterbos & Greenawalt 1996, Xu & Helou 1996b) were based on the assumption that this dust population model is also valid for M31, the $60/100/175\ \mu\text{m}$ triplet provides a direct clue for the validity of this fundamental assumption – at least for the large and small dust grains.

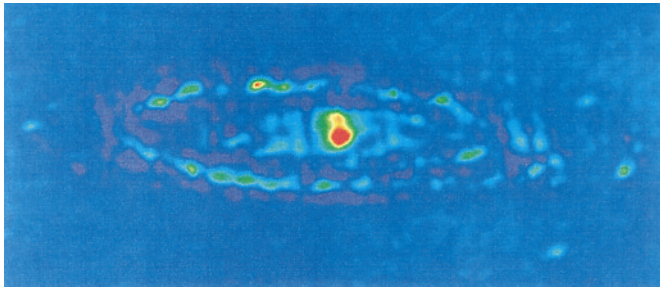


Fig. 5. 100 μm –175 μm difference map of M31, aligned along the major axis. Before computing the difference, the IRAS high resolution 100 μm and ISO 175 μm maps were normalised by their total flux and smoothed to the same spatial resolution (2'.5 FWHM). The difference map spatially separates the cold areas (violet) from the cool/warm/very-warm ones (green/yellow/red), zero level = blue.

However, with respect to the unidentified dust carriers, PAHs and HACs, about which we cannot draw a conclusion from our data, mid-infrared spectra (Cesarsky et al. 1998, Lequeux et al. 1998) indicate that M31 is still different from the Milky Way.

The luminosity of M31's 16 K cold dust component alone is $L_{8-1000\mu\text{m}} = 2.1 \cdot 10^9 L_{\odot}$, while that of all components including the IRAS 12 and 25 μm data is $3.3 \cdot 10^9 L_{\odot}$ which is about 40% higher than former estimates (Xu & Helou 1996a).

Since the temperature of the cold dust component is now well known, its mass can be derived via its emission yielding $3 \cdot 10^7 M_{\odot} \pm 30\%$ (using the formula between luminosity, temperature and mass: $M_{\text{dust}} = 6 \cdot 10^3 \{L_{8-1000}/10^8 L_{\odot}\} \{T_{\text{dust}}/40\text{K}\}^{-6} M_{\odot}$ derived from Hildebrand, 1983, with 0.1 μm mean grain size). This is even higher than the value of $2.4 \cdot 10^7 M_{\odot}$ previously inferred by Xu & Helou (1996b) via their sophisticated emission-extinction model with considerable assumptions and extrapolations. For comparison the IRAS data alone (dotted curve in Fig. 4) would yield a dust mass of only $2.8 \cdot 10^6 M_{\odot}$, about ten times lower than our value. The mass of the 45 K warm component is negligible ($10^5 M_{\odot}$) and we refer now only to the cold dust mass.

The new value of $3 \cdot 10^7 M_{\odot}$ brings the dust-to-HI-gas ratio to about 1/130, close to the value 1/170 for the Milky Way, thereby resolving a former discrepancy. M31's FIR luminosity and dust mass is only about 20% and 50% of that for the Milky Way ($11 \cdot 10^9 L_{\odot}$, $5.7 \cdot 10^7 M_{\odot}$, Sodroski et al. 1994). In total mass and in the blue light, however, M31 is surpassing the Milky Way by a factor of two and 1.6 (see Hodge 1990).

M31's opacity can now be derived from the dust mass where we adopt that a dust column density of $0.1 M_{\odot} \text{pc}^{-2}$ corresponds to an optical depth of $\tau_V \approx 0.5$. Distributing the dust mass uniformly within a thin slab of 10 kpc radius yields a face-on optical depth of $\tau_V \approx 0.5$. For the ring with a diameter 10 kpc and width of 1 kpc which contains about half of the dust mass the optical depth increases to $\tau_V \approx 1.2$, while the dense cloud complex located 5' northwest of the nucleus reaches an average face-on optical depth of $\tau_V \approx 2.5$ (from $3.7 \cdot 10^6 M_{\odot}$, area 0.72 kpc^2),

which at high inclination might still increase. Our extinction values, though locally somewhat higher, agree with the radial average values found by Xu & Helou (1996b) via their extinction model ($\tau_V \approx 0.7-1.6$, inclination 77°). Thus, the dust layer appears to be optically thin or of only moderate optical thickness over most of the disk of M31. However, in the 10 kpc ring area the disk may be optically thick or, alternatively, the cold dust grains are preferentially distributed in isolated dense clumps. In the latter case, although giving an equal amount of FIR emission, the effective optical thickness for transmission of light is substantially smaller than for a homogeneous distribution of dust.

Acknowledgements. We thank the referee Françoise Combes for constructive criticism. The development and operation of ISOPHOT and the data reduction are supported by funds from Deutsches Zentrum für Luft- und Raumfahrt (DLR, formerly DARA).

References

- Arp, H. 1964, ApJ 139, 1045
 Beck, R.; Gräve, R. 1982 A&A 105, 192
 Bothun G.D.; Rogers, C. 1992, AJ 103, 1484
 Braun R. 1991, ApJ 372, 54
 Brinks, E., Shane, W. 1984, ApJS 31, 439
 Buta, R.; Combes, F. 1996, Fundamentals of Cosmic Physics 17, 95
 Buta, R.; van Driel W.; Braine J.; Combes F.; et al. 1995 ApJ 450,593
 Cesarsky D.; et al. 1998, A&A in press
 Desert, F.-X.; Boulanger, F.; Puget, J.L. 1990, A&A 237, 215
 Devreux, N.A.; Price, R.; Wells, L.A.; Duric, N. 1994, AJ 108, 1667
 Disney, M.J.; Davies, J.I.; Phillips, S. 1989, MNRAS 239, 939
 Fruchter, A.S.; Hook, R.N. 1997, Applications of Digital Image Processing XX, Proc. SPIE, Vol. 3164, ed. A. Tescher, p. 120
 Habing et al. 1984, ApJ Letters 278, L59
 Hildebrand, R.H. 1983, Quart. J. Royal. Astron. Soc. 24, 267
 Hodge, P. 1990, "The Andromeda Galaxy", Kluwer Academic Publishers, Dordrecht 1992
 Hoernes, P.; Berkhuijsen, E.M.; Xu, C. 1998 A&A 334, 57
 Hook, R.N. et al. 1994, ST-ECF Newsletter, No. 21, p.16
 Laureijs R. et al., 1998, ISOPHOT Data User Manual, V4.0
 Lemke, D. et al. 1996, A&A 315, L64
 Lequeux J.; et al. 1998, A&A submitted
 Odenwald, S.; Newmark, J.; Smoot, G. 1998, ApJ 500, 554
 Pellet, A. et al. 1978, A&AS 31, 439
 Sodroski, T.J. et al. 1994, ApJ 428, 638
 Sofue, Y.; Kato, T. 1981, Publ. Astron. Soc. Japan 33, 449
 Soifer, B.T.; Houck, J.R.; Neugebauer, G. 1987, ARAA 25, 187
 Stark, A.A. 1977, AJ 213, 368
 Tesesco, A. 1993, "Galaxies in the Infrared" in: Infrared Astronomy eds. A. Mampaso, M. Prieto, F. Sanchez, Cambridge Univ. Press
 van den Bergh, S. 1991, PASP 103, 1053
 Valentijn, E. 1990, Nature 346, 153
 Walterbos, R.A.M.; Greenawalt, B. 1996, ApJ 460, 696
 Walterbos, R.A.M., Kennicutt, R. 1988, A&A 198, 61
 Walterbos, R.A.M.; Schwering, P.B.W. 1987, A&A 180, 27
 Xu, C.; Helou, G. 1996a, ApJ 456, 152
 Xu, C.; Helou, G. 1996b, ApJ 456, 163